THE JOURNAL OF PHYSICAL CHEMISTRY C

Article

pubs.acs.org/JPCC

Sulfur and Silicon Doping in Ag_3PO_4

Pakpoom Reunchan*[,†,‡] and Naoto Umezawa[†,§,∥]

[†]Environmental Remediation Materials Unit, National Institute for Materials Sciences, Ibaraki 305-0047, Japan

[‡]Department of Physics, Faculty of Science, Kasetsart University, Bangkok 10900, Thailand

[§]PRESTO, Japan Science and Technology Agency (JST), 4-1-8 Honcho Kawaguchi, Saitama 332-0012, Japan

[∥]TU-NIMS Joint Research Center, School of Materials Science and Engineering, Tianjin University, 92 Weijin Road, Nankai District, Tianjin, P.R. China

Supporting Information

ABSTRACT: Silver orthophosphate (Ag_3PO_4) is known as a highly active visible-light sensitized photocatalyst, yet its doping effects on electric properties have not been well understood. Using hybrid density-functional calculations, we study possibilities for *n*-type and *p*-type doping in Ag_3PO_4. It is found that a sulfur substituted for phosphorus (S_P) has a relatively low formation energy (high solubility) and acts as a shallow donor in any growth conditions examined. Whereas, a substitutional silicon at phosphorus site (Si_P) is a deep acceptor and its solubility is low, indicating that *p*-type conductivity is unlikely to occur by Si doping. Our results suggest that sulfur doping is a promising approach for the realization of *n*-type Ag_3PO_4.

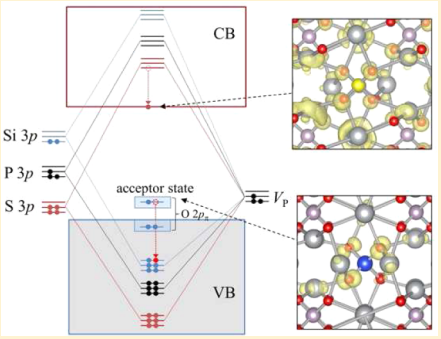

1. INTRODUCTION

Photocatalysis has become an important technology for sustainable environment and clean energy production.[1] Titanium dioxide (TiO_2) has long been used as semiconductor photocatalyst because of its strong oxidizing potential and durability. However, TiO_2 can utilize only ~5% of solar energy because of its wide band gap of 3.0−3.2 eV. Doping with impurities in such a way to improve its absorption into visible-light region is widely used. Unfortunately, dopants also often act as carrier recombination centers, and thus decrease the photocatalytic activities and thereby quantum efficiency. Recently, silver-based oxides semiconductors, such as Ag_3VO_4,[2] $AgGaO_2$,[3] and $AgAlO_2$,[3,4] are found to show photocatalytic activities under visible-light irradiation. One advantage of silver-based oxide is the formation of a multicharacter valence band consisting of Ag d and O p states, which increases hole mobility[5] and is thereby likely to promote oxidation reactions. In particular, Ag_3PO_4 has shown to yield very high quantum efficiency of nearly 90% for the evolution of O_2 from water under visible light irradiation.[6] Combination of its band gap of 2.45 eV (direct) and appropriate position of valence-band (VB) edge as well as its band character makes Ag_3PO_4 suitable for photocatalytic oxidation reaction, and become a prototype for visible-light responsive photocatalyst. This triggers further studies on the properties and applications of Ag_3PO_4 by means of experiments[7−10] and density-functional (DFT) calculations.[10−14]

In a photoelectrochemical cell, *n*-type and/or *p*-type semiconductors are required as either photoanode and/or photocathode, respectively, so that the photoelectrolysis can occur (once the band edges of the semiconductor straddle the redox potentials for the reduction/oxidation reactions). The use of two different semiconductors with suitable band edges position as anode (*n*-type) and cathode (*p*-type) is known to give higher electron−hole potential which enhances the desired chemical reactions.[15] Such chemical reactions occurring at the surface of semiconductor photocatalyst could also be affected by the properties of semiconductor, for instance carrier concentration and the Fermi level. The *n*-type conductivity can be also beneficial for enhancing oxidation reactions due to the upward band bending toward water solution. As-grown Ag_3PO_4 was suggested to be an *n*-type semiconductor as indicated by the positive photocurrent at anodic potential.[6] The *n*-type characteristic of the thin film was possibly caused by donor impurities, which are unintentionally incorporated into the material during synthesis. However, the stability of the *n*-type characteristic is still questionable. In fact, our comprehensive study of native defects in Ag_3PO_4 suggested that the Fermi level locates in the middle of the band gap and there is no intrinsic carrier conductivity in any equilibrium growth condition,[14] similar to the case in classical semiconductors such as silicon. This is a very different characteristic from the typical photocatalyst, TiO_2, which exhibits *n*-type conductivity without external doping. The free electrons induced by native defects act as "hole killers" and cause the difficulty in achieving a *p*-type TiO_2. Since there are no net carriers induced by native defects in Ag_3PO_4, we expect the external doping is relatively easy in this semiconductor. Indeed, enhancing carrier concentration

Received: September 25, 2014
Revised: December 12, 2014
Published: January 6, 2015

DOI: 10.1021/jp509715b
J. Phys. Chem. C 2015, 119, 2284−2289

and controlling electrical properties of Ag_3PO_4 offer opportunities to improve its photocatalytic activity and also to develop a visible-responsive semiconductor.

An approach to increase electron carriers is doping Ag_3PO_4 with an impurity that provides excess electron in its dominant form. In principle there are three choices for *n*-type doping which are (1) substituting Ag^+ with a divalent impurity, such as Zn and Cd, (2) substituting P^{5+} with hexavalent impurity such as S and Se, and (3) substituting O^{2-} with a heptavalent impurity such as F. In a similar fashion, *p*-type doping might be achieved by doping with impurities that create absence of electron. However, only two options are left because Ag^+ is monovalent. Substitution of P^{5+} or O^{2-} with tetravalent or pentavalent impurities such as Si or N are the possible options. Neither theoretical nor experimental studies on *n*-type/*p*-type doping in Ag_3PO_4 have been reported.

Here we perform hybrid density-functional calculations to investigate the effect of S and Si impurities on the electronic properties of Ag_3PO_4, focusing on their suitability as *n*-type and *p*-type dopants. In this study, S and Si were selected as the candidates for the doping because they are adjacent to P in the Periodic Table, and their atomic radii are just slightly different (Si: 1.18 Å, P: 1.10 Å, and S: 1.03 Å), suggesting that they could be feasibly incorporated on the P site. We first discuss the likelihood of incorporating S and Si into Ag_3PO_4 lattice, later the electronic structures of energetically favorable configurations of S and Si are presented. We find that S and Si are favorably incorporated on the P site where S_P acts as a shallow donor with high solubility, and Si_P is a deep acceptor. Possibility of obtaining *n*-type and *p*-type Ag_3PO_4 are discussed. Finally, we elucidate that Si_P is unlikely to be an effective *p*-type dopant using carrier concentration analysis.

2. COMPUTATION METHOD AND DETAILS

Our calculations are based on density functional theory with the Heyd−Scuseria−Ernzerhof hybrid functional (HSE),[16] as implemented in the VASP code.[17] In the HSE, the screening parameter of the nonlocal Hartree−Fock (HF) exchange is set at 0.2 $Å^{-1}$ (HSE06).[18] The HF mixing parameter of 33% was used to produce a band gap of 2.45 eV, in good agreement with the experimental value of 2.45 eV. For the bulk calculations, a 4 × 4 × 4 Monkhorst−Pack *k*-point set is used for the Brillouin zone integrations. The energy cutoff of 300 eV is used for the planewave expansion. The calculated lattice constant a = 6.05 Å is also in good agreement with the experimental value of 6.005 Å. Our calculations of defects were performed by using 128-atom supercell. A shifted 1 × 1 × 1 Monkhorst−Pack *k*-point set is used for the Brillouin zone integrations. We confirmed that the increase of the *k*-point sampling up to 2 × 2 × 2 does not affect our conclusion. All atoms were relaxed by minimizing Hellmann−Feynman force to less than 0.02 eV/Å.

To determine the likelihood of incorporating an impurity in Ag_3PO_4, we compute its formation energy. For S on the P site, the formation energy is given by

$$E^f(S_P^q) = E_{tot}(S_P^q) - E_{tot}(Ag_3PO_4) - \mu_S + \mu_P + q(\varepsilon_F + \varepsilon_v) \quad (1)$$

where $E_{tot}(S_P^q)$ is the total energy of a Ag_3PO_4 supercell containing one S_P in charge state q, and $E_{tot}(Ag_3PO_4)$ is the total energy of the same supercell with no defect. ε_F is the Fermi level, referenced to the valence-band maximum (VBM), ε_v. The alignment of the averaged electrostatic potential in the supercell with and without defect was applied to ε_v. The P atom that is removed from its site is placed in a reservoir with energy μ_P, referenced to the energy of solid phosphorus (orthorhombic). The μ_P represents the chemical potential of P and can be varied within the region determined by the formation enthalpy of Ag_3PO_4 [$\Delta H_f(Ag_3PO_4)$; calculated value is −10.02 eV] and by the conditions that prevent the precipitation of unwanted compounds such as P_2O_5 and Ag_2O. μ_S represents chemical potential of S, which is derived from the energy of bulk SO_2; which gives the upper bound for $\mu_S = (E_{tot}(SO_2) - 2\mu_O)$. Similarly, in the case of Si doping, μ_{Si} is derived from the energy of bulk SiO_2. The P-rich (O-poor) and P-poor (O-rich) growth conditions, which correspond to the chemical potential settings (μ_{Ag}, μ_P, μ_O)(see Supporting Information), were selected to address the likelihood of S and Si dopants.

3. RESULTS AND DISCUSSION

We find that S atom prefers to occupy the P site over Ag or interstitial sites. The calculated formation energies for S substituting for P (S_P) is much lower than that for S substituting for Ag (S_{Ag}) and for S interstitial (S_i) under both growth conditions for the entire range of Fermi-level considered (see Supporting Information). Sulfur substituting for oxygen is not considered here because S and O are isovalent, and thus S_O is electrically inactive. Similarly, based on calculated formation energies, Si_P is most energetically favorable compared to Si_{Ag} and Si_i (see Supporting Information). We omit Si_O because the large size mismatch between Si and O atoms should result in very high formation energy and thus its concentration in the material can be reasonably negligible.

Figure 1(a) shows the projected density of states (PDOS) of the S, P, and Si 3*p* orbitals and 2*p* orbitals of their surrounding O for the model structures of S_P, P_P, and Si_P. The PDOS of S_P, P_P, and Si_P are properly aligned by using the averaged electrostatic potential of the host constituents that represent the bulk-like region (located far away from the substitutional P sites). The associated electron distributions for the bonding states of the S−O, P−O, and Si−O bonds are shown in the insets. We find the bonding states derived from the *p* orbitals of S, P, and Si and the four surrounding O are located at ∼8.60, ∼6.84, and ∼5.76 eV below the VBM, respectively. This order of the energy levels of bonding states is consistent with their atomic orbital ionization energies (E_{aoi}) where E_{aoi}(S) > E_{aoi}(P) > E_{aoi}(Si) for the 3*p* orbitals.[19] The qualitative understanding of the electronic structure of S_P and Si_P can be gained from the molecular diagram illustrated in Figure 1b. Removal of a phosphorus ($3s^2$ $3p^3$) atom with five valence electrons gives rise to the four dangling bonds from the neighboring oxygen atoms, which combine into the fully occupied a_1-like state (*s* character) and partially occupied triply degenerate t_2-like states (*p* character)[10] (three electrons are from neighboring O atoms). Thus, the t_2-like states can accept five more electrons to yield the sp^3 hybrid orbitals. Sulfur ($3s^2$ $3p^4$) and silicon ($3s^2$ $3p^2$) atoms have six and four valence electrons and the occupation of the vacancy site results in the electronic structures with one electron excess and missing with respect to the nondoped case, respectively. We focus only on the p orbitals involved in the sp^3 hybridization in the following discussion for simplicity. The 3*p* orbitals of S, P, or Si with four, three, and two electrons hybridize with the triply degenerate half filled P vacancy (V_P) states with three electrons missing (three holes). This hybridization gives rise to the bonding state located in the

DOI: 10.1021/jp509715b
J. Phys. Chem. C 2015, 119, 2284−2289

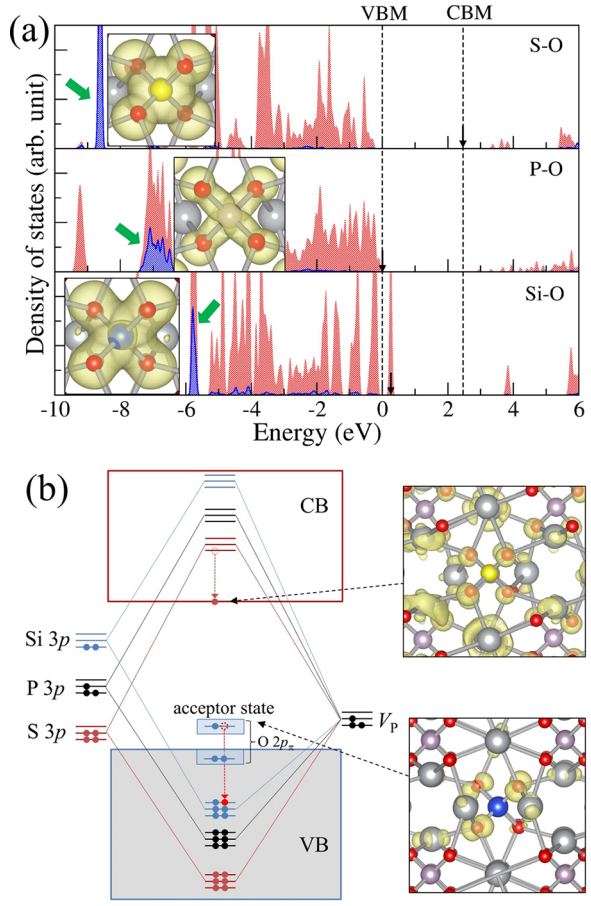

Figure 1. (a) Projected density of states (PDOS) of S, P, and Si 3*p* orbitals (blue shaded) and 2*p* orbitals (red shaded) of the four nearest O atoms for S_P, P_P, and Si_P in the neutral charge state. The insets show the charge distribution of the bonding state associated with S−O, P−O, and Si−O bonds, which are indicated by the solid green arrows. The highest occupied state is schematically shown by the vertical black arrows. (b) Schematic diagram for the interaction between 3*p* orbitals of S, P, or Si with the *p* orbitals of P vacancy (V_P) in S_P, P_P, and Si_P in Ag_3PO_4. The solid dots represent the electron occupation. The charge distributions of the bottom of the conduction band in S_P and of the acceptor state which is located above the valence band (VB) in Si_P are also shown. The isosurfaces in all cases are set to about 90% of the maximum of the respective charge densities.

valence band (VB) and antibonding state located in the conduction band (CB).

We find that S_P introduces no state in the band gap. Four electrons from S can fill the three holes in V_P forming a complete set of S−O bonding states in $(SO_4)^{3-}$ while an extra electron which would occupy the antibonding state transferred to the conduction band minimum. The charge distribution of the conduction-band like state with the extra electron of S_P^0 is depicted in Figure 1b. The delocalization of the electronic charge density indicates that S_P^0 can be readily ionized into S_P^+, describing a characteristic of shallow donor. While three electrons from P can compensate for the three holes in V_P completing the P−O bonding states in $(PO_4)^{3-}$ of nondoped Ag_3PO_4, leaving the CB unoccupied. Two electrons from Si are not sufficient to fully compensate for the three holes in V_P leaving one hole in the system upon the formation of Si−O bonding states in $(SiO_4)^{3-}$ of Si-doped Ag_3PO_4. In the case of Si_P, therefore, an electron is spontaneously transferred from the top of the valence band, which comprises of O $2p_\pi$ and Ag 4*d* states,[10] to the Si−O bonding state. This causes the localization of a hole carrier at oxygen sites near the Si, leading to an upward shift of an O $2p_\pi$ states forming a deep acceptor level. This is consistent with the charge distribution of this acceptor state showing the character of O $2p_\pi$ and Ag 4*d* orbitals (Figure 1b).

Given that S is to the right of P in the Periodic Table, its atomic radius is very close to that of P. We thus expect that S can be easily incorporated into the P site and act as a donor. This is evident from the calculated formation energies of S_P shown in Figure 2. The low formation energy of S_P even under

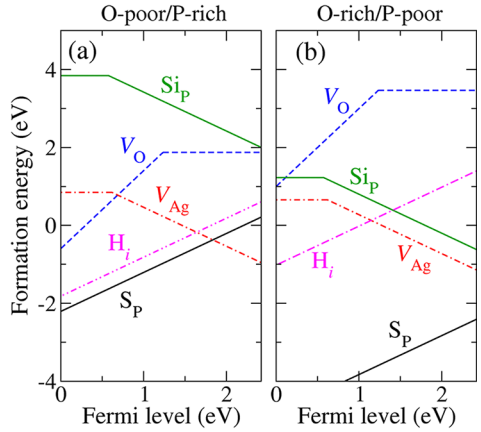

Figure 2. Formation energies as a function of the Fermi level for S_P, Si_P V_O, V_{Ag}, and H_i under (a) O-poor/P-rich and (b) O-rich/P-poor limits. Only the charge states with the lowest formation energy are shown for each value of Fermi level.

P-rich growth condition (Figure 2a) shows that S is very likely to substitute for P. This can be attributed to the slightly smaller atomic size of S compared to that of P, and strong binding with oxygen atoms observed as the deeper bonding state of S−O than of P−O (Figure 1a). The substitution of P by S leads to a slight relaxation of the local lattice around S_P; the four nearest-neighbor O atoms relax inward by 4.6% of the equilibrium P−O bond length. Under P-poor (O-rich) growth condition (Figure 2b), the formation energy of S_P is much lower than that under P-rich condition, and becomes negative in the entire range of ε_F value in the band gap. Note that, in practice, however, the chemical potential of sulfur in synthesizing S-doped Ag_3PO_4 can be lower than our estimation if precursors are properly selected. We believe that there exists an optimum growth condition for the incorporation of S into P sites in Ag_3PO_4 at which a realistic concentration of sulfur (a positive formation energy of S_P) is achieved in S-doped Ag_3PO_4.

The thermodynamic transition level[20] from S_P^+ to S_P^0, $\varepsilon(+/0)$, is estimated to be at 3.22 eV above the VBM, which is located ~0.8 eV above the CBM; in other word, S_P can be fully ionized even under room temperature. For S_P^+, we find no deep states in the band gap while the extra electron of S_P^0 occupies the bottom of the conduction band (Figure 1b). Combined with a low formation energy discussed above, we conclude that S_P acts as a shallow donor in Ag_3PO_4.

On the other hand, although the atomic radius of Si which is to the left of P in the Periodic Table is only slightly larger than that of P, the substitution of P by Si is not readily attainable. The relatively high formation energy of Si_P compared to S_P even under the P-poor growth condition indicates that the

DOI: 10.1021/jp509715b
J. Phys. Chem. C 2015, 119, 2284−2289

incorporation of Si is much harder than that of S into Ag_3PO_4 possibly due to the higher bonding state of Si−O than of S−O (Figure 1). The solubility of Si_P is likely limited by the formation of SiO_2 which is very energetically preferable. The Si_P in the negative and neutral charge state leads to the outward relaxation of the four nearest O atoms by 6.5% and 5.8%, respectively, yielding, Si−O bond lengths similar to those observed in bulk SiO_2.[21]

The $\varepsilon(0/-)$ transition level for Si_P is located at 0.58 eV above the VBM, indicating that Si_P acts as a deep acceptor; only a small amount of holes is introduced in the valence band even at room temperature. The deep-acceptor behavior of Si_P can be explained by the hole localization on the neighboring O atoms as shown in Figure 1b. Under the P-rich or O-poor limit, the formation energy of Si_P is very high even when ε_F close to the CBM (*n*-type condition), implying that the formation of Si_P is negligible. The decrease of P chemical potential from the P-rich to the P-poor increase the likelihood of Si_P formation by several orders of magnitude (2.6 eV lower in $E^f(Si_P)$). However, the question arises whether as to the deep-acceptor behavior of Si_P can yield sufficient free holes to the valence band. The compensation by native point defects that act as "hole killer" can also degrade *p*-type conductivity of Si doped Ag_3PO_4. Next, we discuss the possibility of *n*-type and *p*-type doping in Ag_3PO_4 with S and with Si in terms of Fermi level position and carrier concentration.

For S doping, it is shown that S_P is dominant over other forms and acts as a shallow donor, yielding full ionization even at room temperature. Moreover, it has very high solubility even under the P-rich limit (Figure 2a). On the basis of the calculations of native defects in Ag_3PO_4 reported by the authors,[14] only probable acceptor defect which would act as "electron killer" is Ag vacancy (V_{Ag}). On the other hand, hydrogen interstitial (H_i) is the most energetically favorable donor impurity which can be unintentionally incorporated into the materials during growth. In an intrinsic case, the Fermi level should be determined by a charge neutrality condition where negative (V_{Ag}^- and electrons) and positive (H_i^+ and holes) species are balanced, and it nearly corresponds to the intersection of the two lines of V_{Ag} and H_i formation energy plots (Figure 2). By doping with S_P which is a shallow donor with lower formation energy than that of H_i, the Fermi level is shifted toward the conduction band as understood from the fact that the intersection of the lines for S_P and V_{Ag} locates higher in Fermi level than that of H_i and V_{Ag}. This is true for both the P-rich and P-poor conditions. Here, we assumed that V_{Ag} and H_i act as an acceptor and donor, respectively, even though they are very mobile and possibly annealed out from the bulk region.[14] In such a case when V_{Ag} is incapable of activating hole carriers, the likelihood of *n*-type conductivity on the formation of S_P is rather increased due to the absence of the compensation center. In any case, therefore, the Fermi level of S-doped Ag_3PO_4 is significantly shifted upward compared to the intrinsic case, yielding very high electron concentration. We therefore believe that *n*-type Ag_3PO_4 is achievable by S doping.

On the other hand, doping Ag_3PO_4 *p*-type is much more challenging because of the following points. (1) The solubility of Si_P is fairly low. (2) Si_P is a deep acceptor with a transition level $\varepsilon(0/-)$ 0.58 eV above the VBM which means that only a very small fraction of Si_P(~1.73×10^{-8} %) contributes to free holes in the valence band at room temperature. (3) The acceptor Si_P^- can be compensated for by V_O^{2+}, which has relatively low formation energy under a certain growth condition. We neglect the mobile species V_{Ag} and H_i in the following discussion in order to investigate the best chance for $(Si_P)^-$ to become a source of *p*-type conductivity. On the other hand, the migration barrier of V_O is expected to be relatively high because of a strong covalent bonds in $(PO_4)^{3-}$ and thus is considered to be a major "hole killer" below. In Figure 2, it is shown that the formation energy of Si_P^- decreases while that of V_O^{2+} increases when the oxygen chemical potential, or in other word, oxygen partial pressure varies from the O-poor to the O-rich limits. This implies that in order to increase the number of free holes a growth condition that yield the highest solubility of Si_P and the smallest concentration of V_O^{2+} is needed.

Figure 3 shows the calculated equilibrium concentration of V_O^{2+}, Si_P^-, and hole in the valence band (n_h) for the growth

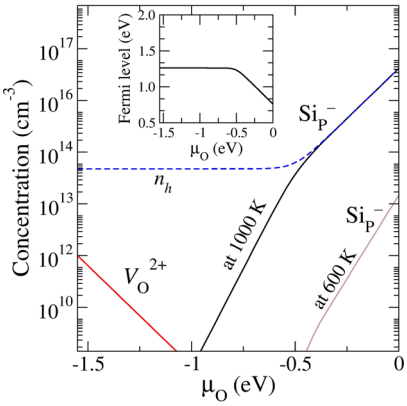

Figure 3. Equilibrium concentration of Si_P^-, V_O^{2+}, and hole in the valence band (n_h) as a function of oxygen chemical potential μ_O for the growth temperature of 1000 K. The inset shows the pinned Fermi level as a function of μ_O. Concentration of Si_P^- for the growth temperature of 600 K is also depicted.

temperature of 1000 K as a function of O chemical potential μ_O. We find that the V_O^{2+} concentration is relatively low (~10^{12} cm^{-3}) even at the O-poor limit ($\mu_O = -1.60$ eV) and becomes lower than that of Si_P^- when $\mu_O > -0.98$ eV, implying that V_O^{2+} is unlikely to act as hole-killer defect. Hole concentration remains steady at ~10^{14} cm^{-3} for a lower μ_O and begins to spontaneously increase when $\mu_O > -0.67$ along with the increased Si_P^- concentration. The Fermi level of Si-doped Ag_3PO_4 is determined by the charge neutrality condition $\sum_i q_i c(X_i^{q_i}) - n_e + n_h = 0$, where n_e and n_h are electron concentration in the conduction band and hole concentration in the valence band defined by $n_e = 2(m_e kT/2\pi\hbar^2)^{3/2} \exp((\varepsilon_F - E_g)/kT)$, $n_h = 2(m_h kT/2\pi\hbar^2)^{3/2} \exp(-\varepsilon_F/kT)$, where m_e and m_h are the electron and hole effective masses of bulk Ag_3PO_4, respectively (calculated m_e and m_h are $0.43m_0$ and $1.11m_0$; m_0 is free electron mass). E_g is the band gap of Ag_3PO_4. $c(X_i^{q_i})$ is the concentrations of X_i defect or impurity in charge state q_i, which includes Si_P and V_O in their corresponding charge states. Here, we assume that the mobile defect and impurity, V_{Ag} and H_i, are annealed out and do not contribute to the charge neutrality. If they are taken into account, there is no chance for Si_P to shift the intrinsic Fermi level (1.62 and 1.15 eV above VBM for O-poor and O-rich, respectively).[14] The inset of Figure 3 shows the Fermi level as a function of μ_O. As μ_O increases the Fermi level decreases and is eventually pinned at ~0.78 eV above the VBM at the O-rich limit. We note that the scenario described above is for the hypothetical growth temperature of 1000 K

DOI: 10.1021/jp509715b
J. Phys. Chem. C 2015, 119, 2284−2289

which is rather high for the calcination temperatures applied to Ag_3PO_4.[22] For the lower growth temperature, e.g., at 600 K, Si_P^- concentration is 3 orders of magnitude lower (see Figure 3) and thus the Fermi level should stays at the intrinsic level near the midgap region, resulting in an insulating Ag_3PO_4. In fact, a good *p*-type material has much higher carrier concentration ($\sim 10^{19}-10^{20}$ cm^{-3})[23] and higher growth temperatures are needed to realize such a concentration, which may beyond the melting point of Ag_3PO_4.

Our analysis based on the assumption of thermodynamic equilibrium where the concentrations of the dopants are sufficiently low (dilute limit) and S_P and Si_P are assumed to be isolated. Experimentally, it is often that the growth of materials is deviated from thermodynamic equilibrium. Moreover, it is difficult to incorporate S and Si into Ag_3PO_4 by postgrowth process because the P−O bonds are very strong and it costs much energy to insert those dopants into PO_4 matrix. The postgrowth doping might be possible, however, by advanced doping methods such as laser doping technique.[24] Replacing $(PO_4)^{3-}$ by $(SO_4)^{2-}$ or $(SiO_4)^{4-}$ might be somewhat easier, but feasibility of such substitution must be carefully examined experimentally. Nevertheless, the sufficiently high calcination temperature in the growth processes should warrant the validity of the use of equilibrium approach. To our knowledge, there are no experimental reports for *n*-type and *p*-type external doping in Ag_3PO_4. Only recently, the study of doping by Bi^{3+} for enhancing the photocatalytic activity has been reported.[25] Our study sheds light on the physics of doping at acid ligands and suggests a promising dopant (S_P) for high electron carrier concentration in Ag_3PO_4.

4. CONCLUSION

In summary, we have performed hybrid-density functional calculations to investigate S and Si doping in Ag_3PO_4. We find that both S and Si are energetically favorable to substitute on P site. S_P is found to act as a shallow donor and has a very high solubility, while Si_P behaves as a deep acceptor and its solubility is relatively low which results in a low concentration of hole carriers. Our results suggest that *n*-type Ag_3PO_4 can be feasibly achieved by S-doping whereas fabricating *p*-type Ag_3PO_4 by Si doping is much more difficult.

■ ASSOCIATED CONTENT

Supporting Information

Detailed calculations of the bulk properties of Ag_3PO_4, the chemical potentials used in the calculation, band structure, and the formation energies of S- and Si-related defects. This material is available free of charge via the Internet at http://pubs.acs.org.

■ AUTHOR INFORMATION

Corresponding Author

*(P.R.) E-mail: pakpoom.r@ku.ac.th. Telephone: +66-2-562-5555#3532.

Notes

The authors declare no competing financial interest.

■ ACKNOWLEDGMENTS

We would like to thank J. Cao, H. Abe, and J. Ye for their support and discussions. N.U. thanks H. Hosono and F. Shimojo for fruitful discussion and advice. This work was supported by the Japan Science and Technology Agency (JST) Precursory Research for Embryonic Science and Technology (PRESTO) program. P.R. was supported by Faculty of Science Kasetsart University, Kasetsart University Research and Development Institute (KURDI) and Institute for Promotion of Teaching Science and Technology (DPST Research Grant 036/2557). P.R. thanks S. Limpijumnong for his advice. P.R. and N.U. thank the High-Performance Computing Center of California NanoSystems Institute (CNSI, UCSB) and the Synchrotron Light Research Institute (SLRI, Thailand) for their hospitality.

■ REFERENCES

(1) Tong, H.; Ouyang, S.; Bi, Y.; Umezawa, N.; Oshikiri, M.; Ye, J. Nano-Photocatalytic Materials: Possibilities and Challenges. *Adv. Mater.* **2012**, *24*, 229−251.

(2) Konta, R.; Kato, H.; Kobayashi, H.; Kudo, A. Photophysical Properties and Photocatalytic Activities under Visible Light Irradiation of Silver Vanadates. *Phys. Chem. Chem. Phys.* **2003**, *5*, 3061−3065.

(3) Ouyang, S.; Kikugawa, N.; Chen, D.; Zou, Z.; Ye, J. A Systematical Study on Photocatalytic Properties of $AgMO_2$ (M = Al, Ga, in): Effects of Chemical Compositions, Crystal Structures, and Electronic Structures. *J. Phys. Chem. C* **2009**, *113*, 1560−1566.

(4) Ouyang, S.; Zhang, H.; Li, D.; Yu, T.; Ye, J.; Zou, Z. Electronic Structure and Photocatalytic Characterization of a Novel Photocatalyst $AgAlO_2$. *J. Phys. Chem. B* **2006**, *110*, 11677−11682.

(5) Kawazoe, H.; Yanagi, H.; Ueda, K.; Hosono, H. Transparent P-Type Conducting Oxides: Design and Fabrication of P-N Heterojunctions. *MRS Bull.* **2000**, *25*, 28−36.

(6) Yi, Z.; et al. An Orthophosphate Semiconductor with Photooxidation Properties under Visible-Light irradiation. *Nat. Mater.* **2010**, *9*, 559−564.

(7) Bi, Y.; Ouyang, S.; Umezawa, N.; Cao, J.; Ye, J. Facet Effect of Single-Crystalline Ag_3PO_4 Sub-Microcrystals on Photocatalytic Properties. *J. Am. Chem. Soc.* **2011**, *133*, 6490−6492.

(8) Yao, W.; Zhang, B.; Huang, C.; Ma, C.; Song, X.; Xu, Q. Synthesis and Characterization of High Efficiency and Stable Ag_3PO_4/TiO_2 Visible Light Photocatalyst for the Degradation of Methylene Blue and Rhodamine B Solutions. *J. Mater. Chem.* **2012**, *22*, 4050−4055.

(9) Bi, Y.; Ouyang, S.; Cao, J.; Ye, J. Facile Synthesis of Rhombic Dodecahedral AgX/Ag_3PO_4 (X = Cl, Br, I) Heterocrystals with Enhanced Photocatalytic Properties and Stabilities. *Phys. Chem. Chem. Phys.* **2011**, *13*, 10071−10075.

(10) Kahk, J. M.; Sheridan, D. L.; Kehoe, A. B.; Scanlon, D. O.; Morgan, B. J.; Watson, G. W.; Payne, D. J. The Electronic Structure of Silver Orthophosphate: Experiment and Theory. *J. Mater. Chem. A* **2014**, *2*, 6092−6099.

(11) Umezawa, N.; Shuxin, O.; Ye, J. Theoretical Study of High Photocatalytic Performance of Ag_3PO_4. *Phys. Rev. B* **2011**, *83*, 035202.

(12) Ma, X.; Lu, B.; Li, D.; Shi, R.; Pan, C.; Zhu, Y. Origin of Photocatalytic Activation of Silver Orthophosphate from First-Principles. *J. Phys. Chem. C* **2011**, *115*, 4680−4687.

(13) Liu, J. J.; Fu, X. L.; Chen, S. F.; Zhu, Y. F. Electronic Structure and Optical Properties of Ag_3PO_4 Photocatalyst Calculated by Hybrid Density Functional Method. *Appl. Phys. Lett.* **2011**, *99*, 191903−191903.

(14) Reunchan, P.; Umezawa, N. Native Defects and Hydrogen Impurities in Ag_3PO_4. *Phys. Rev. B* **2013**, *87*, 245205.

(15) Nozik, A. J.; Memming, R. Physical Chemistry of Semiconductor−Liquid Interfaces. *J. Phys. Chem.* **1996**, *100*, 13061−13078.

(16) Heyd, J.; Scuseria, G.; Ernzerhof, M. Hybrid Functionals Based on a Screened Coulomb Potential. *J. Chem. Phys.* **2003**, *118*, 8207−8215.

(17) Kresse, G.; Furthmüller, J. Efficient Iterative Schemes for Ab Initio Total-Energy Calculations Using a Plane-Wave Basis Set. *Phys. Rev. B* **1996**, *54*, 11169−11186.

(18) Krukau, A. V.; Vydrov, O. A.; Izmaylov, A. F.; Scuseria, G. E. Influence of the Exchange Screening Parameter on the Performance of

DOI: 10.1021/jp509715b
J. Phys. Chem. C 2015, 119, 2284−2289

Screened Hybrid Functionals. *J. Chem. Phys.* **2006**, *125*, 224106−224105.
(19) Gray, H. B. *Electrons and Chemical Bonding*; W. A. Benjamin: New York, 1965.
(20) Van de Walle, C. G.; Neugebauer, J. First-Principles Calculations for Defects and Impurities: Applications to III-Nitrides. *J. Appl. Phys.* **2004**, *95*, 3851−3879.
(21) Pluth, J. J.; Smith, J. V.; Faber, J. Crystal Structure of Low Cristobalite at 10, 293, and 473 K: Variation of Framework Geometry with Temperature. *J. Appl. Phys.* **1985**, *57*, 1045−1049.
(22) Guo, J.; Ouyang, S.; Li, P.; Zhang, Y.; Kako, T.; Ye, J. A New Heterojunction Ag_3PO_4/Cr-$SrTiO_3$ Photocatalyst Towards Efficient Elimination of Gaseous Organic Pollutants under Visible Light Irradiation. *Appl. Phys. B: Laser Opt.* **2013**, *134−135*, 286−292.
(23) Kawazoe, H.; Yasukawa, M.; Hyodo, H.; Kurita, M.; Yanagi, H.; Hosono, H. P-Type Electrical Conduction in Transparent Thin Films of $CuAlO_2$. *Nature* **1997**, *389*, 939−942.
(24) Eisele, S. J.; Röder, T. C.; Köhler, J. R.; Werner, J. H. 18.9% Efficient Full Area Laser Doped Silicon Solar Cell. *Appl. Phys. Lett.* **2009**, *95*, 133501.
(25) Zhang, S.; Zhang, S.; Song, L. Super-High Activity of Bi^{3+} Doped Ag_3PO_4 and Enhanced Photocatalytic Mechanism. *Appl. Phys. B: Laser Opt.* **2014**, *152−153*, 129−139.

DOI: 10.1021/jp509715b
J. Phys. Chem. C 2015, 119, 2284−2289